

6470
MAY 13 1947

ACR May 1942

Copy 1

RECEIVED
NATIONAL ADVISORY COMMITTEE FOR AERONAUTICS



WARTIME REPORT

ORIGINALLY ISSUED

May 1942 as
Advance Confidential Report

HIGH-SPEED TESTS OF A DUCTED BODY WITH
VARIOUS AIR-OUTLET OPENINGS

By John V. Becker and Donald D. Baals

Langley Memorial Aeronautical Laboratory
Langley Field, Va.

NACA

WASHINGTON

NACA WARTIME REPORTS are reprints of papers originally issued to provide rapid distribution of advance research results to an authorized group requiring them for the war effort. They were previously held under a security status but are now unclassified. Some of these reports were not technically edited. All have been reproduced without change in order to expedite general distribution.

L - 486

NACA LIBRARY
LANGLEY MEMORIAL AERONAUTICAL
LABORATORY
Langley Field, Va.

NATIONAL ADVISORY COMMITTEE FOR AERONAUTICS

ADVANCE CONFIDENTIAL REPORT

HIGH-SPEED TESTS OF A DUCTED BODY WITH VARIOUS AIR-OUTLET OPENINGS

By John V. Becker and Donald D. Baals

SUMMARY

Test of a ducted body with internal flow were made in the 8-foot high-speed wind tunnel for the purpose of studying the effects on external drag and on critical speed of the addition of efficient inlet and outlet openings to a basic streamline shape. Drag tests of a 13.6-inch-diameter streamline body of fineness ratio 6.14 were made at Mach numbers ranging from 0.20 to 0.75. The model was centrally mounted on a 9-percent-thick airfoil and was designed to have an efficient airfoil-body juncture and a high critical speed. An air inlet at the nose and various outlets at the tail were added; drag and internal-flow data were obtained over the given speed range.

The critical speed of the ducted bodies was found to be as high as that of the streamline body. The external drag with air flow through the body did not exceed the drag of the basic streamline shape. No appreciable variation in the efficiency of the diffuser section of the internal duct occurred throughout the Mach number range of the tests.

INTRODUCTION

The tests of ducted bodies reported in reference 1 showed that the external drag of bodies with well-designed air inlet and outlet openings did not exceed the drag of the basic streamline body to which the openings were added. Pressure-distribution and boundary-layer data were presented that satisfactorily accounted for the drag characteristics. Further tests of a ducted fuselage (reference 2) yielded the same results as the tests of reference 1.

The ducted bodies of the tests of references 1 and 2 were supported by 12-percent-thick airfoils, and some local separation of the flow at the airfoil-body junctures

was found to exist and was reported. The airfoils were located near the center of each body, well out of the measurable field of influence of the openings. Nevertheless, it has been suggested that the drag measured with internal air flow might have been affected by the alleviation of the local separated condition at the juncture.

One purpose of the present tests was to compare the drag of a ducted body with the drag of a streamline body under conditions that would be free from any possible interference effects at the airfoil-body juncture. The tests were planned to include several types of outlet opening, to cover a wide range of internal mass-flow coefficients, and to extend to Mach numbers of about 0.75. Pressures were measured at the outlet openings and behind the diffuser section of the duct throughout the range of test Mach numbers in order to determine the internal drag and the diffuser efficiency.

The model employed in these tests has been used in a subsequent investigation employing a heated radiator.

SYMBOLS

V_0	free-stream velocity, feet per second
v	local velocity, feet per second
p	static pressure, pounds per square foot, absolute
ρ	density, slugs per cubic foot
q	dynamic pressure, pounds per square foot ($\frac{1}{2} \rho V^2$)
Δh	total-pressure loss, pounds per square foot
F	maximum cross-sectional area of fuselage, 1.009 square feet
A	area, square feet
Q	quantity of flow, cubic feet per second
$\frac{\rho Q}{\rho_0 F V_0}$	mass-flow coefficient

P pressure coefficient $\left(\frac{P - P_o}{q_o} \right)$
 η_d diffuser efficiency $\left(1 - \frac{\Delta h}{q_1 - q_2} \right)$
 a velocity of sound, feet per second
 M Mach number (v/a)
 C_{D_T} external-drag coefficient

$$\frac{(\text{total drag of combination}) - (\text{drag of wing}) - (\text{drag calculated from internal losses})}{q_o F}$$

x distance from leading edge of respective sections, inches
 y vertical distance, inches
 R outside radius, inches
 R_i inside radius, inches

Subscripts:

o free-stream condition
 1 condition at inlet
 2 condition immediately behind diffuser
 4 condition at outlet

APPARATUS AND METHODS:

Streamline body.— The streamline body of revolution (fig. 1, table I) was derived from a modified version of the NACA fuselage form 111. (See reference 1.) The nose section was designed with a fineness ratio of 4.28 with the maximum thickness at the 24.5-inch station. At this point the nose section faired into a cylindrical center section 12 inches long, designed to increase the critical speed of the wing-body juncture. At the 36.5-inch station a tail section of fineness ratio 6.05 faired into the center

section. The fineness ratio of the resultant body was 6.14. The sections dimensioned in figure 1 represent the parting lines of the nose and tail sections and do not necessarily coincide with the sections used in deriving the model ordinates.

Ducted model.— The nose-inlet profile was derived from nose B of reference 1 and was designed to fair into the streamline body. (See figs. 1 and 2 and table II.) The center section was the same for all model modifications.

Tails A, B, and C were derived from the streamline tail but were cusped at the outlet in accordance with the recommendations of references 1 and 2. (See figs. 1 and 2 and table I.) These outlets were designed for a mass-flow coefficient $\frac{\rho Q}{\rho_0 V_0}$ of about 0.06, 0.0425, and 0.025 for the tails A, B, and C, respectively. The outlet areas are included in table II. Tail D was formed by cutting off the streamline tail to the same length as the cusped tails - A, B, and C. The resultant shape was a straight-walled outlet of converging section with an outlet area of 0.0603 square foot. The partial-annular outlet, tail E, (figs. 1 and 3(a)) was installed in the streamline tail at the 13.65-inch station with the ordinates derived from the proposed optimum shape of reference 2. The outlet area was 0.0587 square foot. The outlet areas of both tails D and E were approximately the same as the outlet area of tail B.

Internal-duct design.— The ducted body was intended to serve not only in the test program reported herein but also in an investigation requiring the installation of a heated radiator. (See reference 3.) The details of the internal-duct design, therefore, were partly governed by the installation details of the radiator.

The diffuser had an equivalent conical expansion angle of 8° back to the 14.75-inch station. At this point the duct expanded more rapidly until the constant-diameter section of $11\frac{3}{16}$ inches was reached. (See fig. 1 and table II for internal-duct ordinates.) For one of the tests with tail B a simulated engine resistance of $\Delta h/q_0 = 0.27$ for $C = 0.0425$ was installed within the diffuser at the 21.50-inch station.

Supporting airfoil.— A thin, relatively small airfoil was used to support the bodies in order both to minimize the interference effects of the juncture and to reduce the tare

drag. The section used was the NACA 66-009. (See fig. 1.) The airfoil contained a duct through which pressure leads were carried outside the tunnel.

Boundary-layer condition. - Boundary-layer transition was artificially fixed both on the wing and near the nose of the fuselage in order to eliminate drag variations caused by the shifting of the transition point and to secure results significant for high Reynolds number applications. Transition was fixed by a 1/4-inch-wide strip of No. 60 carborundum glued to the surface at the 10-percent-chord station of the wing and at the 1 1/2-inch station of the ducted body. Transition on the streamline body was fixed at the 5 1/2-inch station, corresponding to the location of the strip on the ducted model. Except for the carborundum strips, the model was aerodynamically smooth and fair.

Internal flow and pressure measurements. - The internal-mass-flow rate, the total-pressure loss, and the static pressure at the outlets were obtained by means of a 52-tube rake mounted at the tail outlet. The rake was supported at the end of a 1 1/8-inch-diameter hollow tube that extended through the center of the duct and carried the pressure leads from the rake to the wing duct. (See figs. 1 and 3(b).) The blades of the rake were removed during the force tests.

An 8-tube rake of 5 total-pressure tubes and 3 static-pressure tubes, located 1 1/2 inches behind the diffuser, was used to furnish data on the loss in the diffuser.

TESTS

Each configuration was tested through a Mach number range of 0.20 to 0.75 at 0° angle of attack. Drag and internal-flow data were obtained in separate runs because of the necessity of removing the tail-rake blades during the force tests. The internal flow with the partial-annular outlet (tail E) was obtained from readings of the 8-tube internal rake, which was calibrated against the tail rake.

A tuft survey at the airfoil-body juncture was made through a speed range of 90 to 260 miles per hour.

RESULTS AND DISCUSSION

Figure 4(a) shows the comparison of the external drag

of the ducted bodies with tails A, B, and C with the drag of the streamline body through the range of test Mach numbers. Similar comparisons for tail D and the partial-annular outlet, tail E, are shown in figure 4(b). The external drag was obtained by deducting from the total measured body drag the drag calculated from the measured internal momentum losses. A simple method of computing the internal drag for low-speed test conditions is given in reference 1. In the present tests, however, it was necessary to use the more involved formula of reference 3 which is applicable in the case of high-speed compressible flow. Owing to the fact that the internal losses were very small, the internal drag was low (about 3 percent of the drag of the body with tail B, for example).

It will be noted at once (fig. 4) that the external drag of the ducted bodies did not exceed the drag of the streamline body. The tail outlets tested appeared to have only a slight advantage over the partial-annular outlet of tail E. Tail D, with the straight converging sides, had about the same drag as tail B, which was of corresponding size but of cusped contour. Previous tests (references 1 and 2) had shown that, for converging outlets, the external flow was considerably decreased as compared with that of the cusped tail. Tail D, however, did not contract as abruptly as the tails of references 1 and 2 and thus the outlet characteristics corresponded more closely to the outlet characteristics of a tail with a cusped contour.

The tuft survey of the flow in the wing-body juncture verified the expectation that unusually smooth flow conditions existed. For speeds above 260 miles per hour but below the critical speed, no marked change in drag coefficient was found, indicating that similar flow conditions prevailed throughout the subcritical speed range. (See fig. 5.) The drag comparisons made in this paper may, therefore, be considered free from interference effects due to unsatisfactory flow conditions in the wing-body juncture.

Figure 6 shows that the internal-mass-flow coefficient $\frac{\rho Q}{\rho_0 F V_0}$ remained nearly constant with increasing

Mach number. The theory of reference 3 indicates that this coefficient will be constant provided that, as in the present case, the internal losses are small. The very slight increase at the higher speeds is attributed to a reduction of the small duct-friction losses due to

the favorable scale effect and to the favorable compressibility effect described in reference 3.

The pressure coefficients at the cusped-tail outlet are shown in figure 7. Little change occurred with increasing Mach number.

Figure 8 shows the variation of diffuser efficiency with Mach number M_0 for various inlet-velocity ratios. The data show that the diffuser efficiency remains essentially constant throughout the test Mach number range. The diffuser efficiency, however, increases slightly with a decrease in inlet-velocity ratio. This effect may be ascribed to the natural divergence of the streamlines at the inlet opening; the greater divergence corresponding to the lower inlet velocities results in improved flow in the diffuser. A similar result was described in reference 4.

The maximum value of the inlet Mach number M_1 attained in the present tests was 0.45, which can be determined from the tabulated values of inlet velocity ratio v_1/v_0 of figure 8. For inlet velocities of the order of the speed of sound ($M_1 = 1$), the value of the diffuser efficiency will decrease sharply because of the formation of a shock wave within the entrance.

The diffuser efficiency for these tests is defined as

$$\eta_d = 1 - \frac{\Delta h}{q_1 - q_2}$$

This equation becomes identical with the more usual form

$$\eta_d = \frac{p_2 - p_1}{q_1 - q_2}$$

if the flow is incompressible and the velocity distribution is uniform. For compressible flow at high speeds, the ideal static-pressure rise is more rapid than the corresponding dynamic-pressure decrease. The usual definition of η_d in terms of the static and dynamic pressures will, therefore, give meaningless results at high speeds (values of $\eta_d > 1$ in some cases). It is recommended that the definition in terms of the total-

pressure loss

$$\eta_d = 1 - \frac{\Delta h}{q_1 - q_2}$$

be adopted, because this value of η_d does not change measurably with M_0 , as is shown in figure 8.

CONCLUSIONS

For a model on which the wing-body interference was negligible, the external drag of a ducted body with air inlet and outlet openings of suitable shape did not exceed the drag of the basic streamline body to which the openings were added. This result corroborates the conclusions of references 1 and 2.

The critical compressibility speed of the ducted bodies was the same as that of the streamline body.

The diffuser efficiency did not vary appreciably for the Mach number range of these tests.

Langley Memorial Aeronautical Laboratory
National Advisory Committee for Aeronautics,
Langley Field, Va.

REFERENCES

1. Becker, John V.: Wind-Tunnel Tests of Air Inlet and Outlet Openings on a Streamline Body. NACA A.C.R., Nov. 1940.
2. Becker, John V., and Baals, Donald D.: Wind-Tunnel Tests of a Submerged-Engine Fuselage Design. NACA A.C.R., Oct. 1940.
3. Becker, J. V., and Baals, D. D.: The Aerodynamic Effects of Heat and Compressibility in the Internal Flow Systems of Aircraft. NACA A.C.R., Sept. 1942.
4. Patterson, G. N.: Modern Diffuser Design. The Efficient Transformation of Kinetic Energy to Pressure, Aircraft Engineering, vol. 10, no. 115, Sept. 1938, pp. 267-273.

Streamline nose		Center section		Streamline tail	
x	R	x	R	x	R
0	0	0	6.78	0	6.49
.73	1.29	1.5	6.80	3.0	6.25
1.46	1.95	4.5	6.80	6.0	5.92
2.92	2.93	10.5	6.80	9.0	5.52
4.37	3.64	13.5	6.80	12.0	5.06
5.83	4.21	15.5	6.78	15.0	4.52
8.75	5.03	18.5	6.71	18.0	3.94
11.66	5.64	21.5	6.58	21.0	3.35
14.58	6.10	23.0	6.49	24.0	2.75
17.49	6.44			27.0	2.14
20.41	6.67			30.0	1.53
23.00	6.78			33.0	.92
				37.5	0

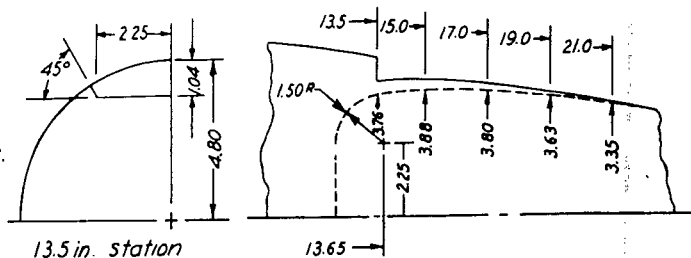
DUCTED-BODY ORDINATES IN INCHES

[illegible]

Airfoil ordinates, NACA 66-009			
x	y	x	y
0	0	8.00	0.888
.10	.139	9.00	.899
.15	.167	10.00	.897
.25	.209	11.00	.881
.50	.282	12.00	.842
1.00	.389	13.00	.782
1.50	.469	14.00	.691
2.00	.535	15.00	.568
3.00	.638	16.00	.444
4.00	.718	17.00	.319
5.00	.782	18.00	.185
6.00	.832	19.00	.074
7.00	.866	20.00	0

Leading-edge radius=0.112

1. Fuselage ordinates given in table I
2. All dimensions in inches.



Partial annular outlet, tail E

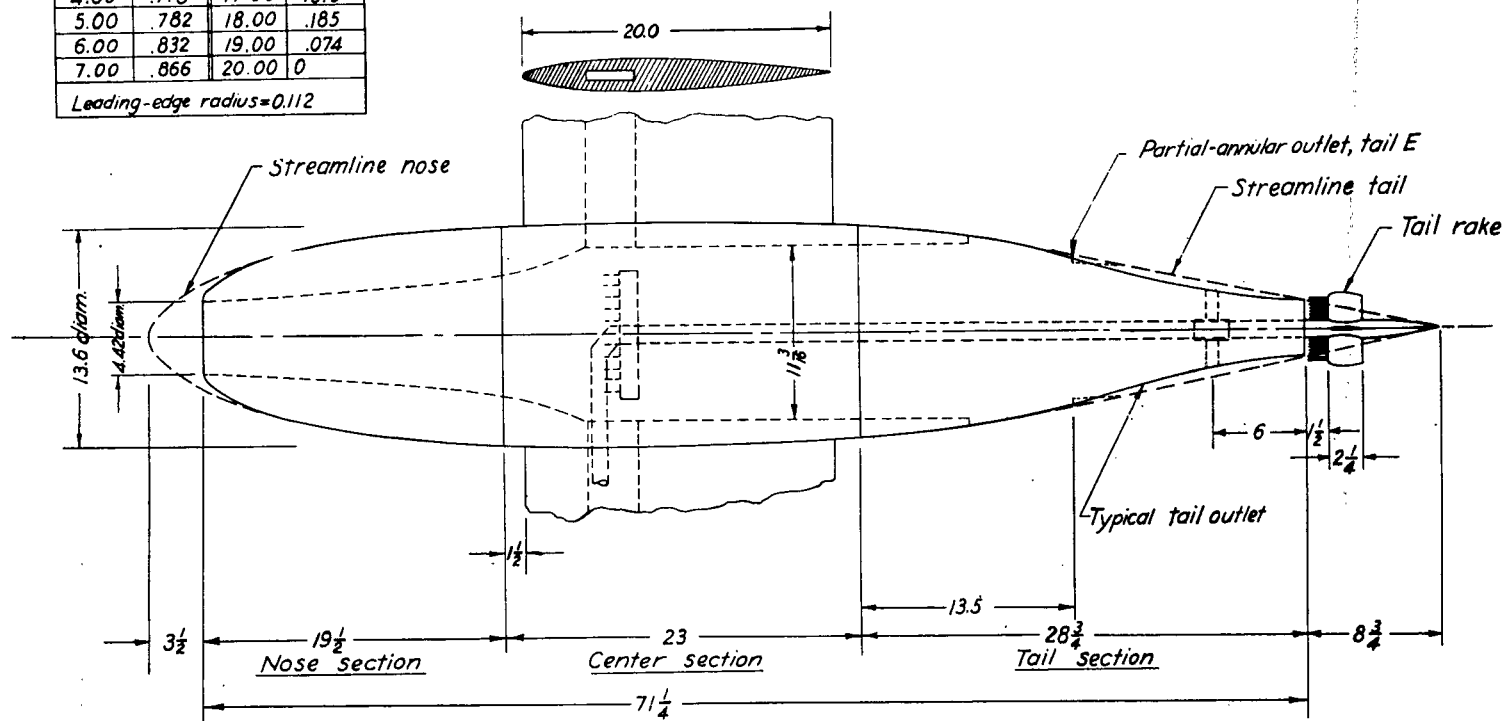


Figure 1.- Model details.



Figure 2.- General view,
ducted body,
tail B.

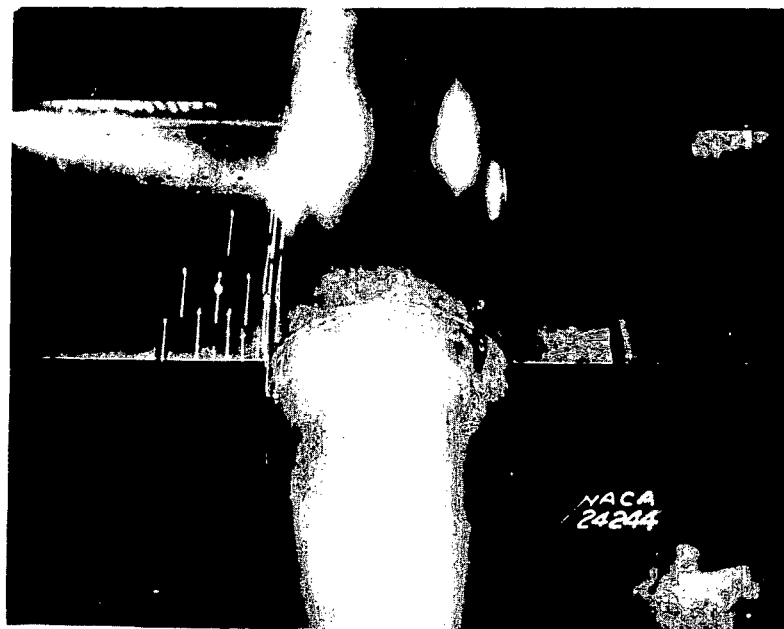
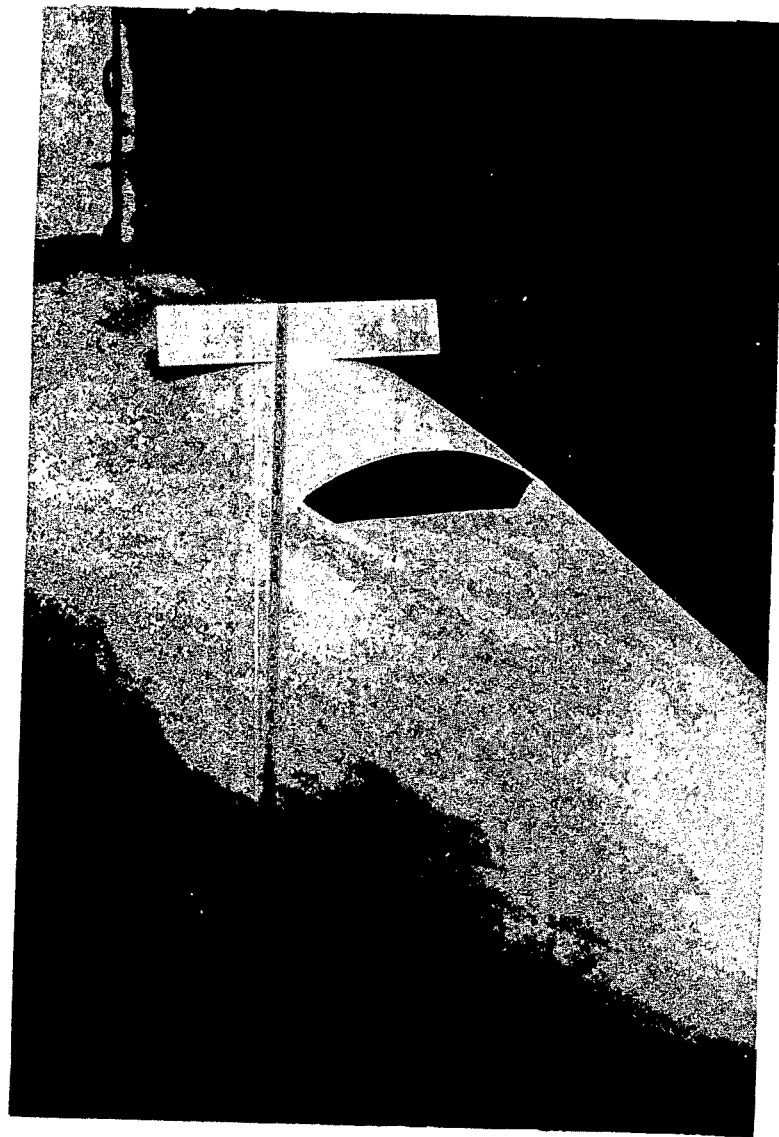
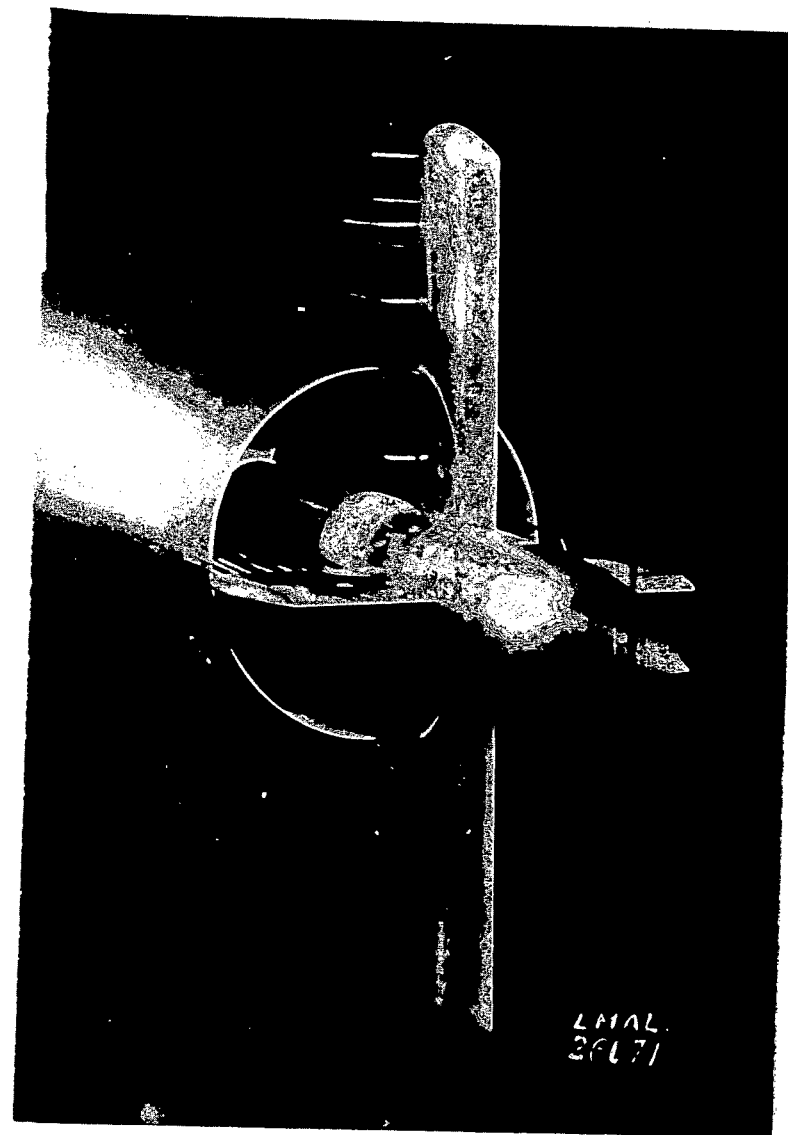


Figure 5.- Flow in wing-
nacelle
junction. M , 0.30.

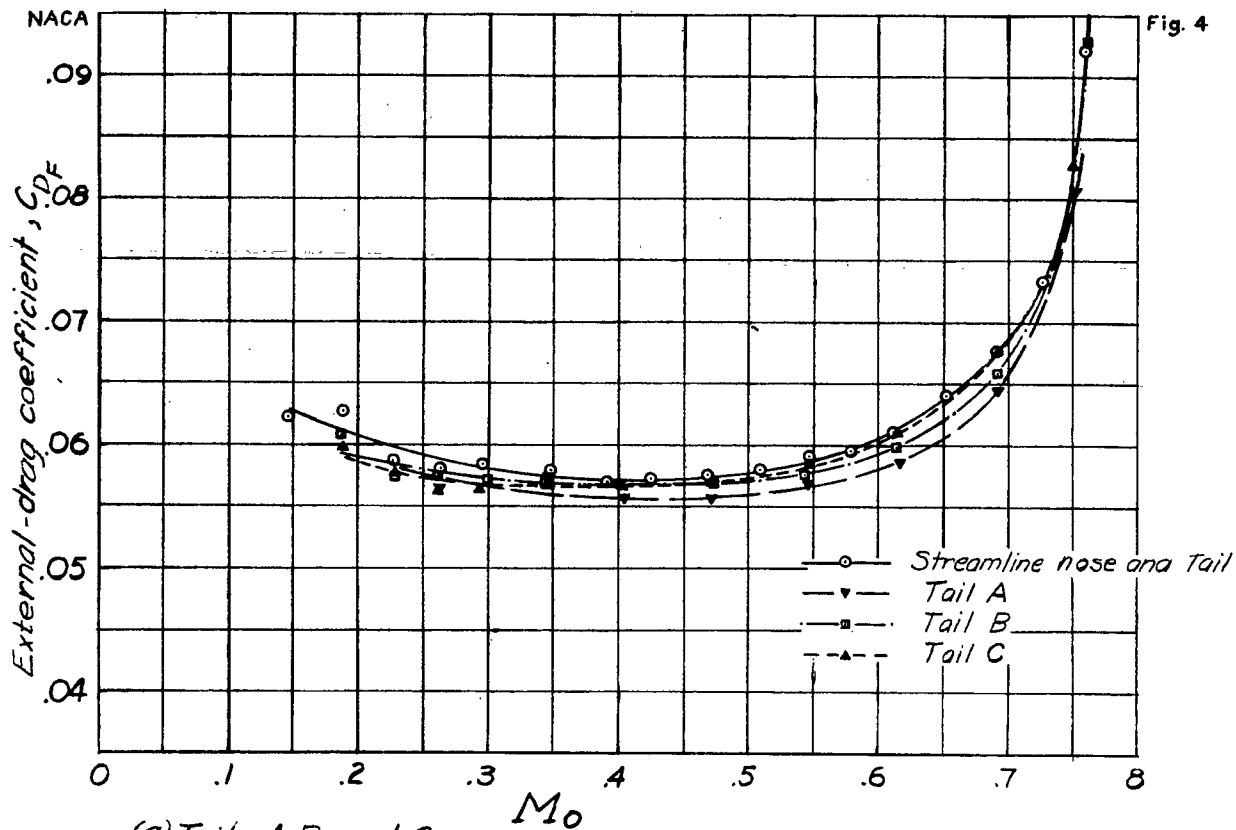


(a) Partial annular outlet, tail E.

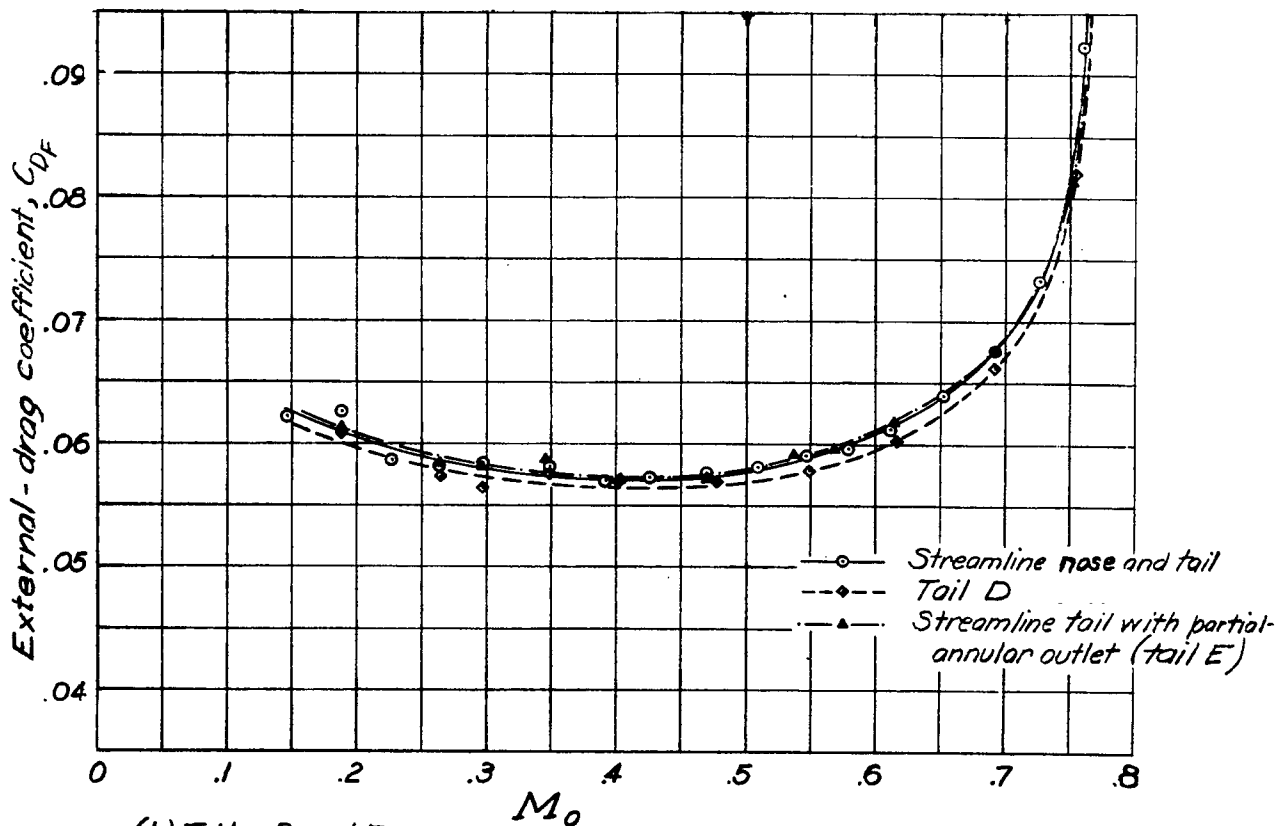


(b) Tail B outlet with tail rake.

Figure 3.- Model outlet details.



(a) Tails A, B, and C.
Figure 4.- Variation of external-drag coefficient with Mach number for various tails.



(b) Tails D and E.

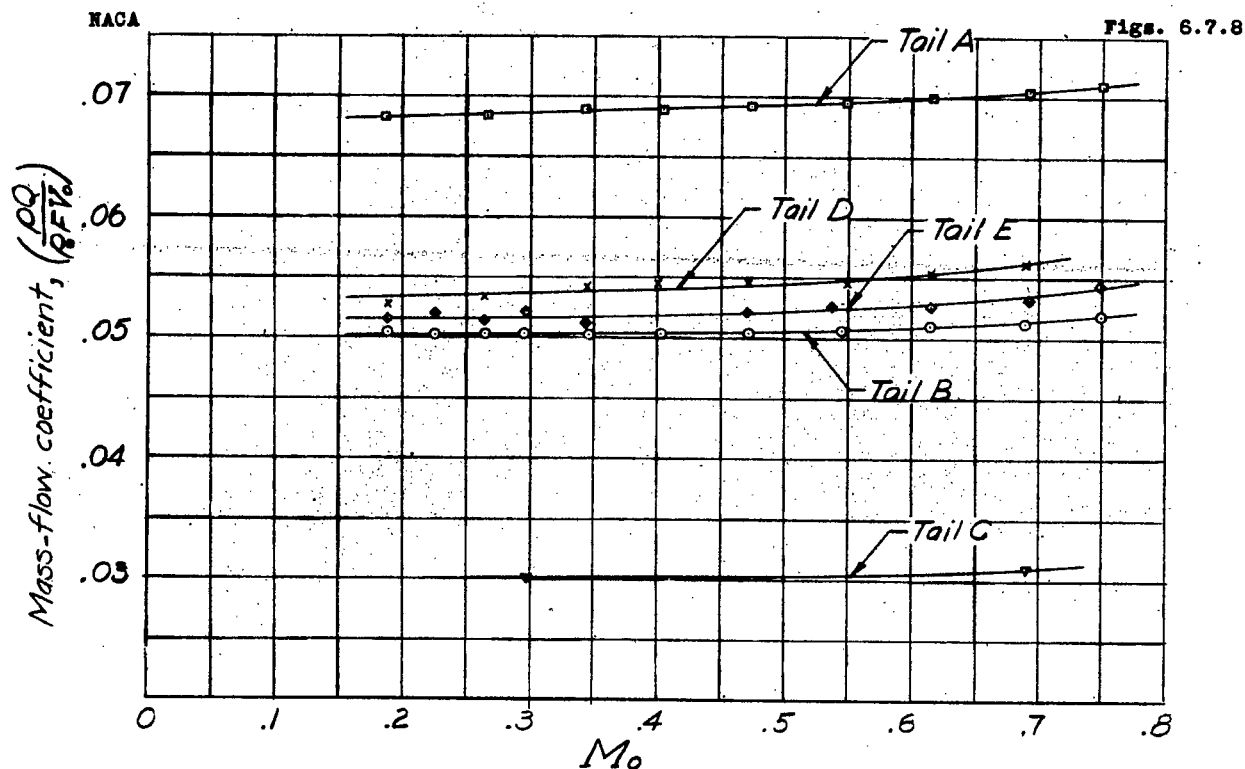


Figure 6.- Variation of mass-flow coefficient with Mach number for various tails.

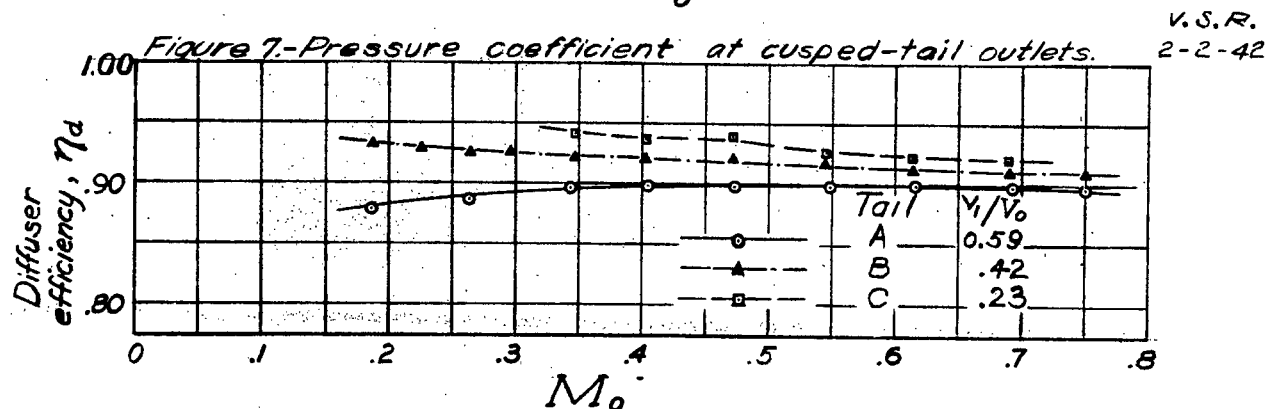
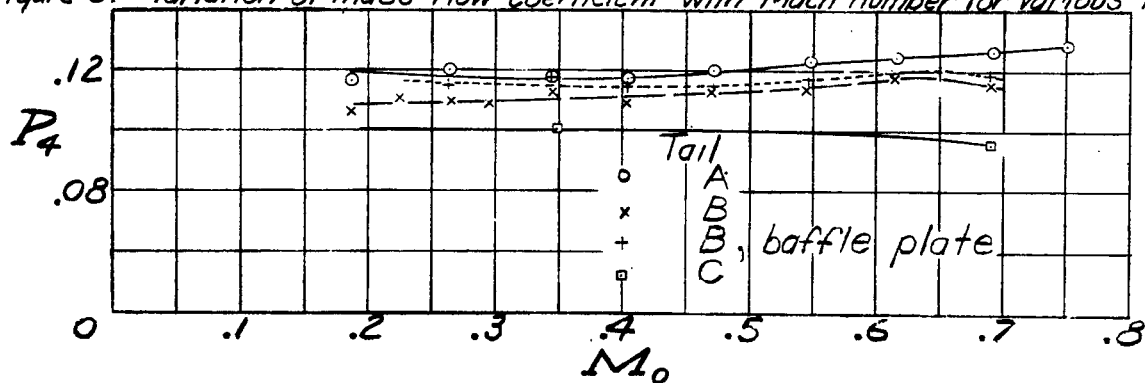


Figure 8.- Variation of diffuser efficiency with Mach number for various inlet-velocity ratios. $\eta_d = 1 - \frac{\Delta h}{q_1 - q_2}$.